U.S. DEPARTMENT OF THE INTERIOR
U.S. GEOLOGICAL SURVEY

A Method of Estimating the Amount of In-situ Gas Hydrates in Deep Marine Sediments

by
M.W. Lee[1], D.R. Hutchinson[2], W.P. Dillon[2],
J.J. Miller[1], W.F. Agena[1], and B.A. Swift[2]

Open-File Report 92-276

[1]U.S. Geological Survey, Box 25046, Denver Federal Center, Denver, CO 80225
[2]U.S. Geological Survey, Woods Hole, MA 02543

Table of Contents

Table of Figures

Table of Tables

ABSTRACT

The bulk volume of gas hydrate in marine sediment can be estimated by measuring interval velocities and amplitude blanking of hydrated zones from true-amplitude processed multichannel seismic reflection data. In general, neither velocity nor amplitude information is adequate to independently estimate hydrate concentration. We propose a method that uses amplitude blanking calibrated by interval-velocity information to quantify hydrate concentrations in the Blake Ridge area of the U.S. Atlantic continental margin.

On the Blake Ridge, blanking occurs in conjunction with relatively low interval velocities. The model that best explains this relation linearly mixes two end-member sediments, hydrated and unhydrated sediment. Hydrate concentration in the hydrate end-member can be calculated from a weighted equation that uses velocity estimated from the seismic data, known properties of pure hydrate, and porosity inferred from a velocity/porosity relationship. Amplitude blanking can be predicted as the proportions of hydrated and unhydrated sediment change across a reflection boundary. Our analysis of a small area near DSDP 533 indicates that the amount of gas hydrates is about 6% in total volume when interval velocity is used as a criterion and about 9.5% when amplitude information is used. This compares with a calculated value of about 8% derived from the only available measurement in DSDP 533.

INTRODUCTION

Below a few hundred meters of water depth in the world's oceans, shallow sea floor sediment lies in the pressure/temperature zone of phase stability for gas hydrates. Gas hydrates are ice-like crystalline solids that are formed of a cage of water molecules surrounding a guest gas molecule. Evidence of their existence has come from recognizing a bottom simulating reflector (BSR) on seismic profiles and sampling by the Deep Sea Drilling Program (DSDP) and Ocean Drilling Program (ODP) (Kvenvolden and Barnard, 1983; Shipley and Didyh, 1982; Suess, von Huene, and others, 1988). In most naturally occurring gas hydrates, the guest molecule is methane.

Even though large volumes of hydrates appear to exist within the upper several hundred meters below the sea floor, no quantitative approaches are known for estimating the amount of in situ gas hydrates. Estimates of the global quantity of methane in hydrates have been presented by many researchers (Dobrynin and others., 1981; McIver, 1981; Kvenvolden, 1988; Sloan, 1990 and references therein); these estimates differ by as much as two orders of magnitude. A limitation of these estimates is the assumption of in-situ conditions and thermodynamic state. Hence, these assessments are neither quantitative nor accurate because they are not based on observable information.

Estimating the amount of gas hydrates contained in marine sediments is important. Hydrates contain perhaps 600,000 to one million TCF of methane (Kvenvolden, 1988), approximately 35,000 to 65,000 times the U.S. gas consumption in 1989. Therefore, hydrates are a potential source of energy, although methods of extracting marine hydrates have not been developed. This large volume may be significant to climate change. Methane has 3.7 times the global warming effect of carbon dioxide on a molar basis (or 10 times on a weight basis, Lashof and Ahuja, 1990). Although CH_4's average residence time in the atmosphere is only about 10 years, it is oxidized to CO_2, which continues to create greenhouse warming (Lashof and Ahuja, 1990). Finally, the dissociation of hydrates in sediments (for example, by lowering sea level) may be one cause of slope failure on continental margins (Dillon and others, in press, Paull and others, 1991).

Gas hydrates are known to increase the interval velocity of sediments (Stoll 1974; Tucholke and others, 1977; Dillon and Paull, 1983), by an amount that is proportional to the amount of hydrate (Pearson and others, 1983). This relation was used by Tucholke and others (1977) to explain an observed variation of velocity in the range of 1.6 to 1.9 km/s by the variable thicknesses of hydrated

sediments. Sheridan, Gradstein and others (1983) estimate that near DSDP 533 (Figure 1), as much as 20 to 30% of the sedimentary section should have been gas hydrate in order to produce an average velocity of 2 km/s, although such large amounts of hydrate were not recovered during drilling.

Another indicator of gas hydrates is the amplitude reduction or blanking typically observed above the BSR in reflection profiles from regions of known hydrates. Shipley and others (1979) related the marked decrease of amplitude above the bottom simulating reflector (BSR) to the presence of hydrates that reduced the impedance contrast across sedimentary interfaces. Dillon and others (in press) also observed amplitude blanking from true-amplitude seismic sections, and ascribe this effect to hydrate formation. These studies imply that amplitude information can be used as an indicator of hydrate cementation.

In this paper, we propose a quantitative method for estimating the amount of gas hydrates in marine sediments based on measurable acoustic properties of seismic reflection data. Our approach utilizes both the kinematics (interval velocity) and the dynamics (seismic amplitude) of the wave field; more specifically, the increase in velocity and decrease in reflection amplitude observed in regions of known hydrate occurrence.

GEOLOGIC SETTING AND BSR

The continental margin of the southeastern United States is a zone of depositional transition between the actively building carbonate platform of the Bahamas and the terrigenous or clastic-dominated shelf-slope-rise configuration of eastern North America (Dillon and Popenoe, 1988). The region off North and South Carolina is the southern limit of the dominantly terrigenous continental margin. In this region, contour-following bottom currents since the Oligocene have built a sediment drift deposit of hemipelagic sediments that extends southeastward away from the continental slope, and forms the Blake Ridge (Figure 1). Seismic profiles over the Blake Ridge and the continental rise just to its north are prominently marked by a large amplitude reflection event that approximately parallels the sea floor, known as the Bottom Simulating Reflector (BSR) (Markl and others, 1970; Ewing and Hollister, 1972; Tucholke and others, 1979; Shipley and others, 1979). The BSR is believed to be caused by a large impedance contrast at the base of the hydrate stability zone which juxtaposes sediment containing gas hydrate with deposits containing free gas.

A primary objective of DSDP site 533 on the Blake Outer Ridge (Figure 1) was to sample gas hydrates in a region of a well-developed BSR. This hole penetrated 399 m beneath the sea floor and terminated in middle Pliocene silty mud (Sheridan, Gradstein and others, 1983). Gas pockets, disrupted sediments, and frothing characterized parts of the recovered cores. The only direct evidence for gas hydrate occurred at 238 m subbottom depth, where a layer several centimeters thick contained frothy sediment with white matlike crystals that rapidly disappeared when exposed to atmospheric conditions (Kvenvolden and Barnard, 1983).

Gas pockets severely hampered the measurement of physical properties; bulk density was estimated at 1.67-1.74 g/cc and porosity from two intervals was estimated at 57-60%. The BSR was estimated to be about 200 m below the bottom of the hole, or about 600 m below the sea floor (Sheridan, Gradstein et al., 1983.) Chemical analysis shows that the gas is derived through microbiological processes rather than thermogenic processes and consists almost entirely of methane. The high rate of sedimentation has ensured the preservation of enough organic matter for the bacterial production of methane (Kvenvolden and Barnard, 1983).

SEISMIC DATA AND PROCESSING

The location of the five multi-channel seismic profiles used for this investigation are shown in Figure 1. They were recorded in the early -to mid-1970's using tuned air-gun arrays of 1,000 - 2,000 in^3 volume. Four of the lines provide 36-fold coverage with 50 m common-mid-

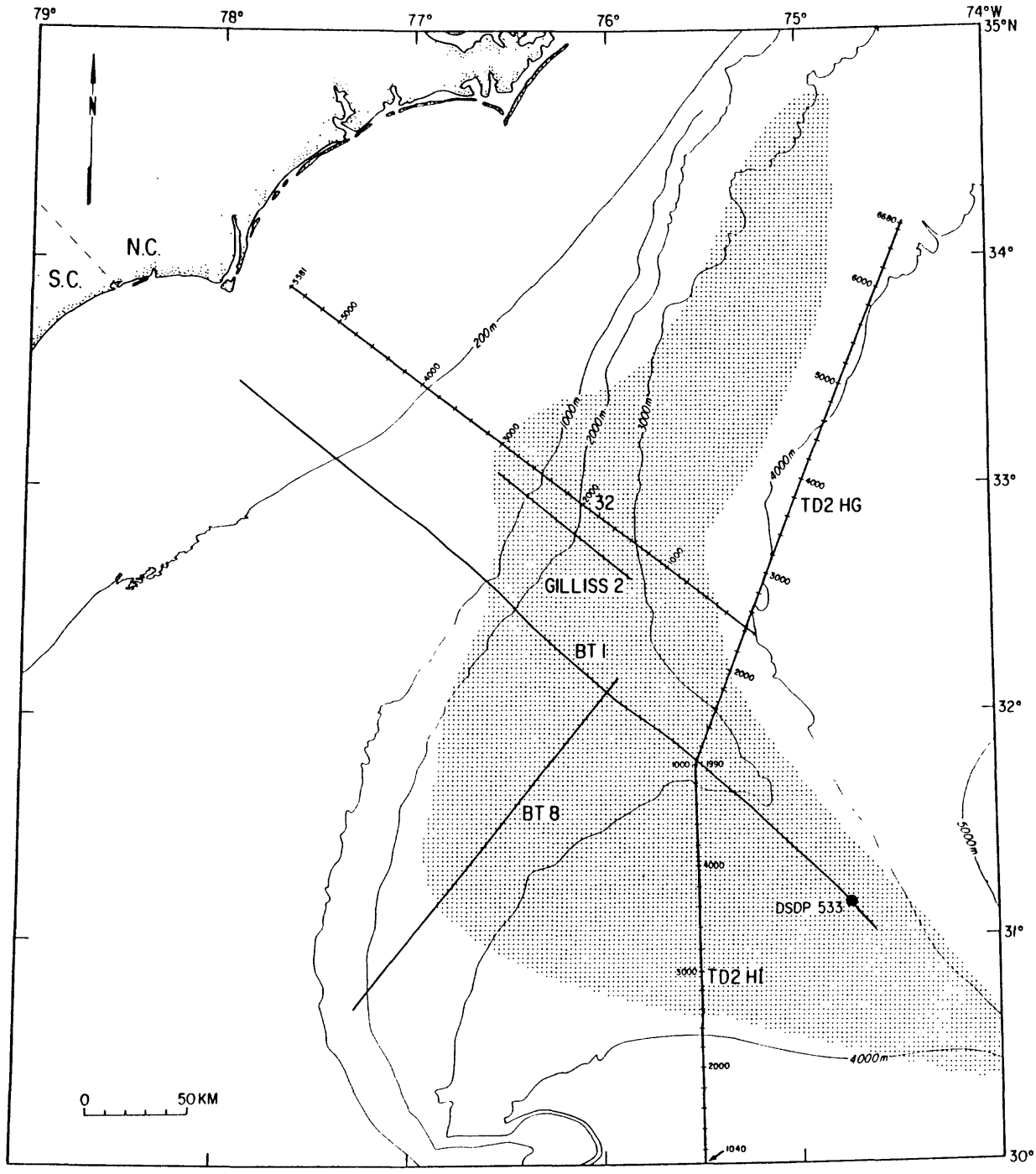

Figure 1. Bathymetry of southeastern U.S. continental margin, location of multichannel seismic reflection profiles, DSDP sites 103, 104, 390, and 533. DSDP 533 was drilled to sample gas hydrate. Bathymetric contours in meters. The dot pattern shows the extent of the Bottom Simulating Reflector (BSR). Modified from Dillon and Popenoe(1988).

point (CMP) intervals. Gilliss 2 is a 12-fold recording (Figure 1). All profiles, except Gilliss 2, were recorded with 48-channel streamers 3.6-km long containing non-linear group spacing. Gilliss 2 was recorded with a linear 1.2-km streamer.

True-amplitude processing

In order to optimize the quantitative analysis of hydrated sediment, a relative true amplitude (RTA) processing technique with wavelet deconvolution was applied to all profiles. The RTA processing was performed by the automatic editing method based on the median amplitude in a CMP gather (Lee and Hutchinson, 1990) with only a spherical spreading correction applied. Other amplitude corrections that compensate for effects such as attenuation and transmission loss were not included in this RTA processing, because these other effects may introduce seismic artifacts that impede the identification of hydrated sediment. Wavelet deconvolution was done by the variable norm deconvolution method (Gray, 1979). A representative source signature from deep water (in the range of two-way traveltimes of 4 s) was derived and an inverse filter was calculated and applied along each line. Source signature variations due to the gun depth, streamer depth, and gun failure were compensated by applying second-zero crossing predictive deconvolution before stack. The justification of this kind of approach, which applies the same inverse filter for the whole profile instead of applying separate deconvolution filters to each gather, comes from the model studies done by Dragoset and others (1987). Examples of wavelet processed seismic data with 6/8 - 40/50 Hz band pass filtering are shown in Figure 2. In this figure, 10 consecutive CMP's are shown for USGS 32 (Figure 2a) and TD2HG (Figure 2b). Both sections show almost symmetrical water-bottom reflections (peak amplitude) and well-defined trough reflections at the BSR. Because of the stacking process, the higher frequency component of data has been lost, but the improvement of signal-to-noise ratio and almost identical wavelets among different seismic lines due to the wavelet processing warrant reliable amplitude analyses of seismic data in this study area. Another example of the wavelet and RTA-processed data for USGS line 32 is shown in Figure 3.

Velocity and Amplitude Analysis

Detailed velocity measurements via stacking analysis were made every 100 CMPs, or about every 2.5 km along profile. Interval velocities determined in this fashion were difficult to estimate in regions of amplitude blanking because reflections are weak and laterally discontinuous. Consequently, in these areas, interval velocities calculated from stacking velocities are not consistently representative of the same geologic interval. We felt a more useful approach was to focus on the average acoustic properties of hydrated sediment, i.e., to measure the average velocity in a zone that extended from the sea floor downward to the BSR (Figure 4), and in another zone about 200 ms above the BSR downward to the BSR. Velocities are average interval velocities calculated from CMP gathers that were selected based on the occurrence of a prominent BSR, the quality of iso-velocity plots of routine stacking velocities, and the seismic character (primarily blanking) of the stacked data.

Our amplitude analysis was also done in these same two zones: either the interval between the sea floor and the BSR, or the 200-ms thick section immediately overlying the BSR. Amplitude changes are based on calculations of the median reflectance which we defined as the absolute value of the reflection coefficient, or the envelope amplitude calibrated by the reflection coefficient. The reflection coefficient can be estimated from the behavior of the water-bottom multiples in the seismic data. Our analysis shows that the water-bottom reflection coefficient decreases with increasing water depth (Lee and others, 1991). The median reflectance calibrated by the reflection coefficient also systematically decreases with increasing water depth. Thus, we correct the median reflectance to a reference water depth, which is arbitrarily set at 3 seconds two-way time(s) in this analysis.

The details of amplitude variation near the BSR can be examined using plots similar to those shown in Figure 5. In those plots, each dot represents the amplitude in an 8 msec window for 5

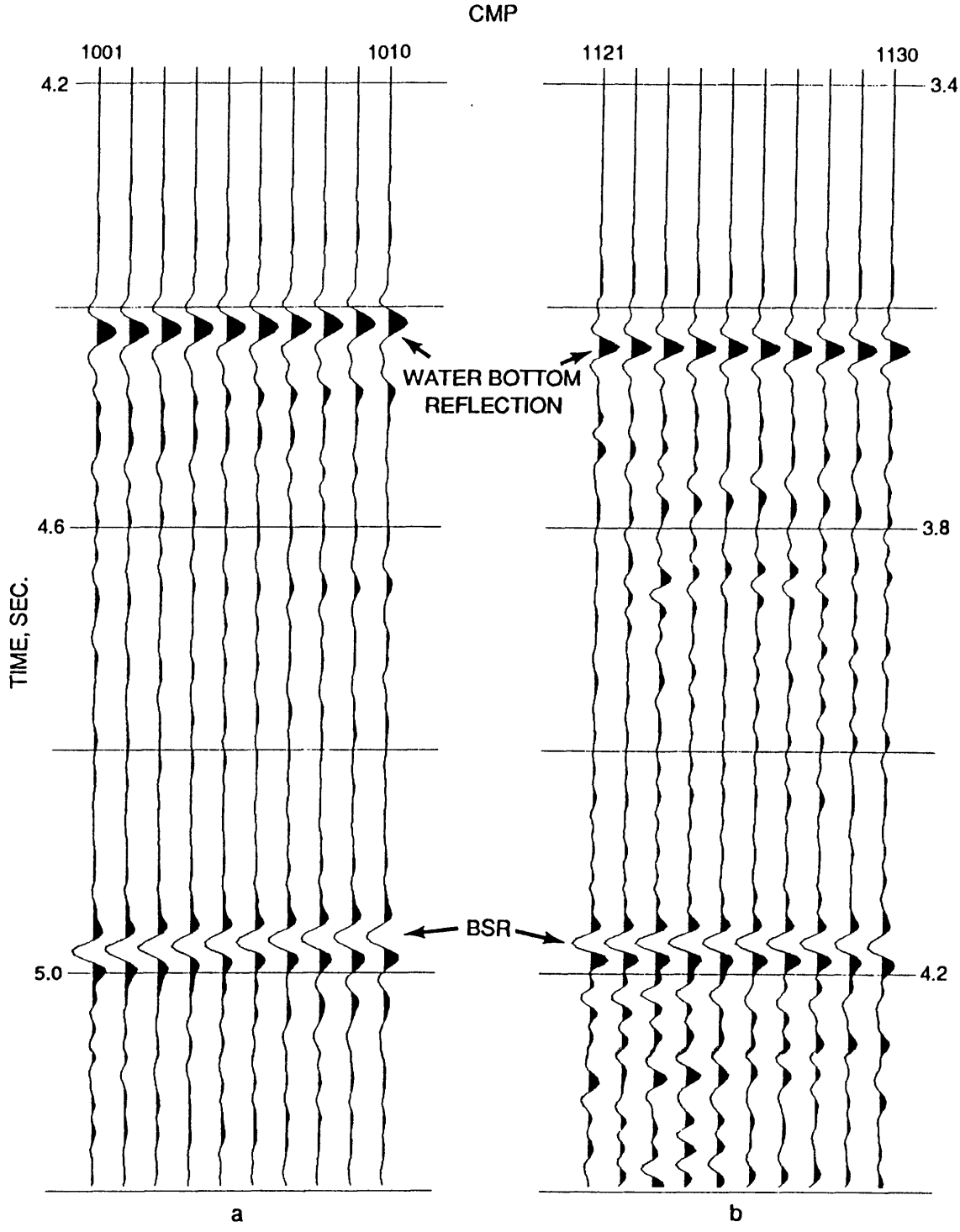

Figure 2. Examples of wavelet processed seismic section. Ten consecutive CMP's are shown. Note the symmetrical peak amplitudes for the water-bottom reflections and the phase reversals at the BSR.
a) USGS 32 and **b)** TD2-HG

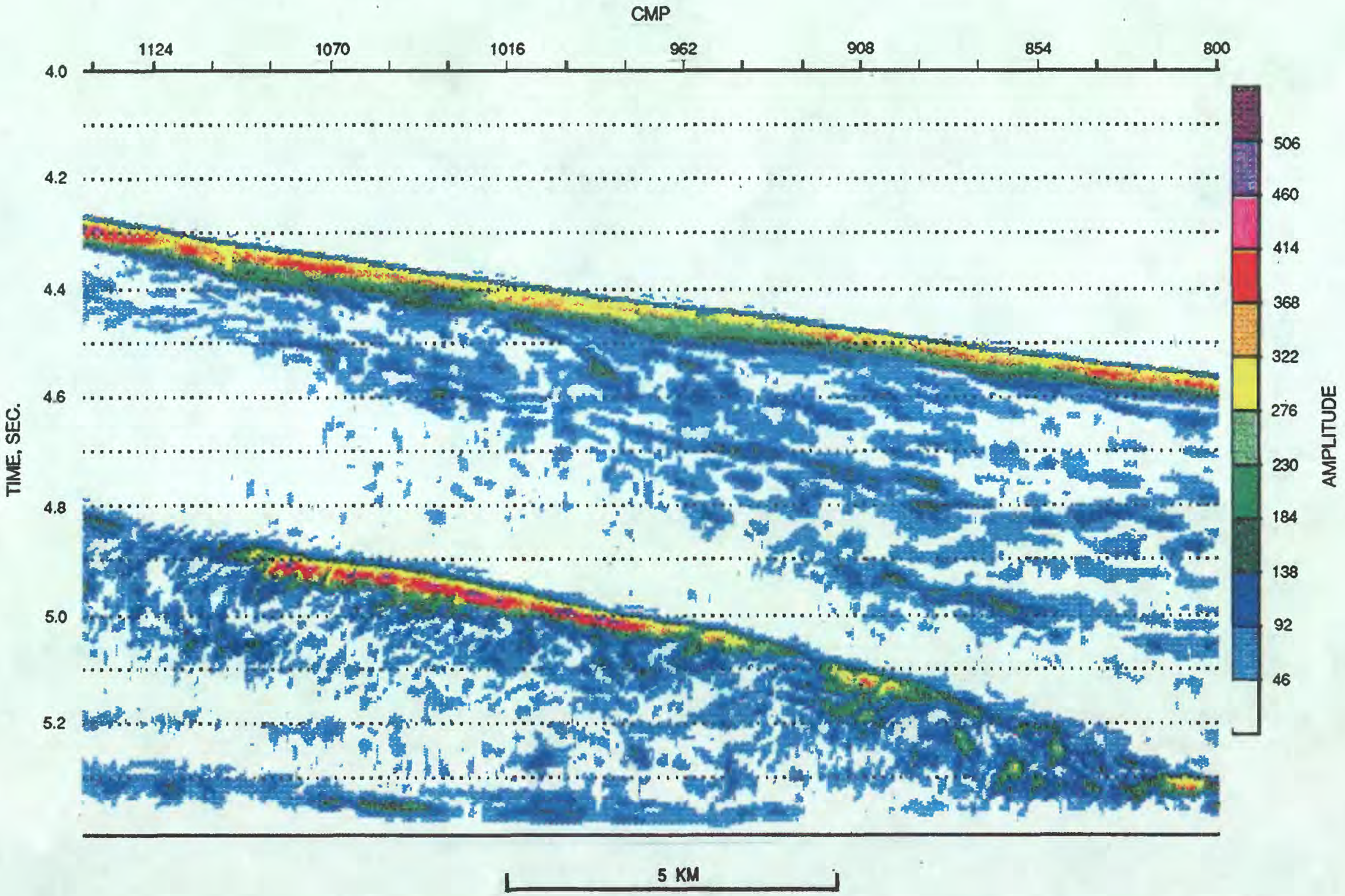

Figure 3. An example of true amplitude processed seismic profile, in color, of a part of USGS line 32. Note the spatial variation of blanking and the high amplitude BSR.

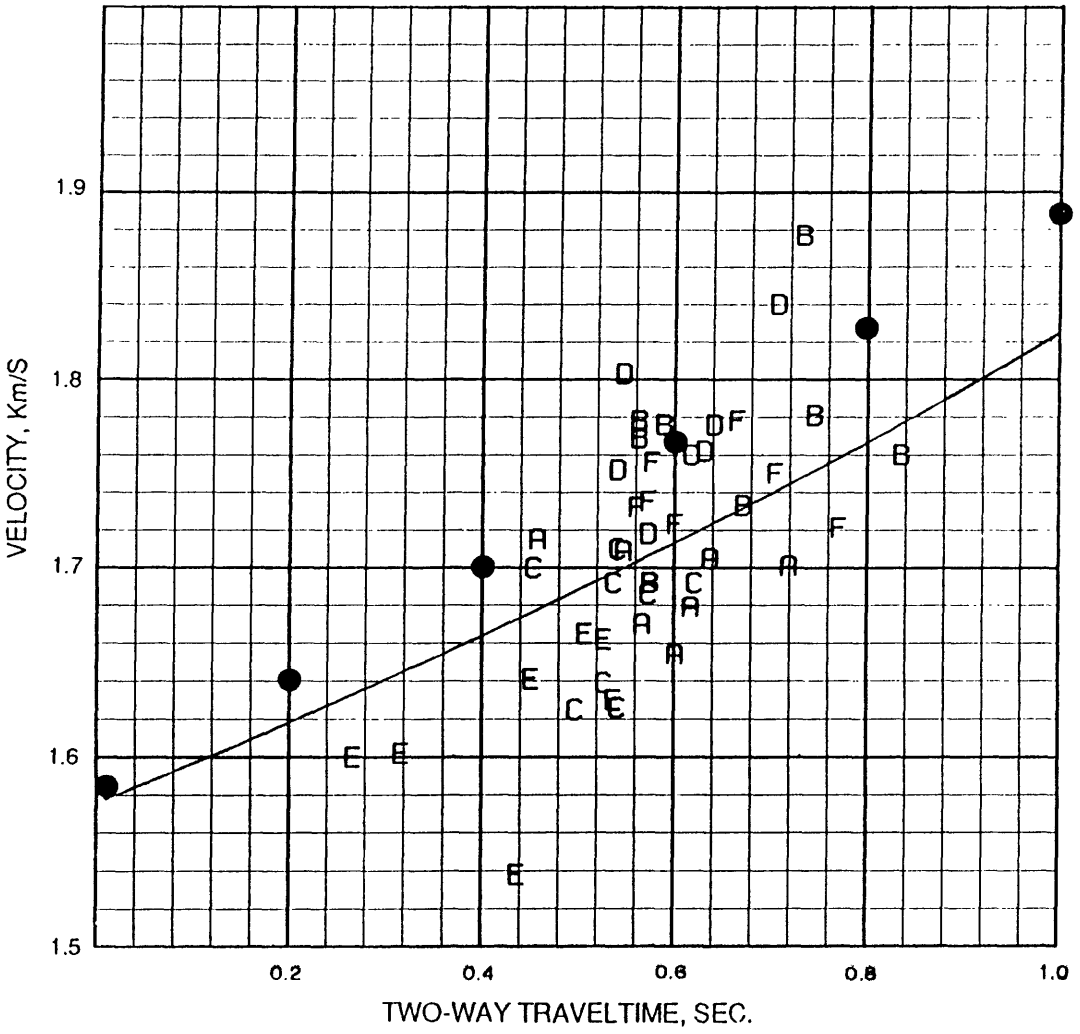

Figure 4. Average interval velocity determined by conventional stacking velocity analysis versus two-way traveltime. The solid line represents the average curve by Carson and others (1986) and the dots represent the average velocity by Houtz (1974). Each letter represents the values of average velocity between the sea floor and the BSR for CMPs along the six seismic profiles: A, B, C, D, E, and F represent TD2HI, TD2HG, BT1, BT8, Gilliss 2, and USGS 32, respectively.

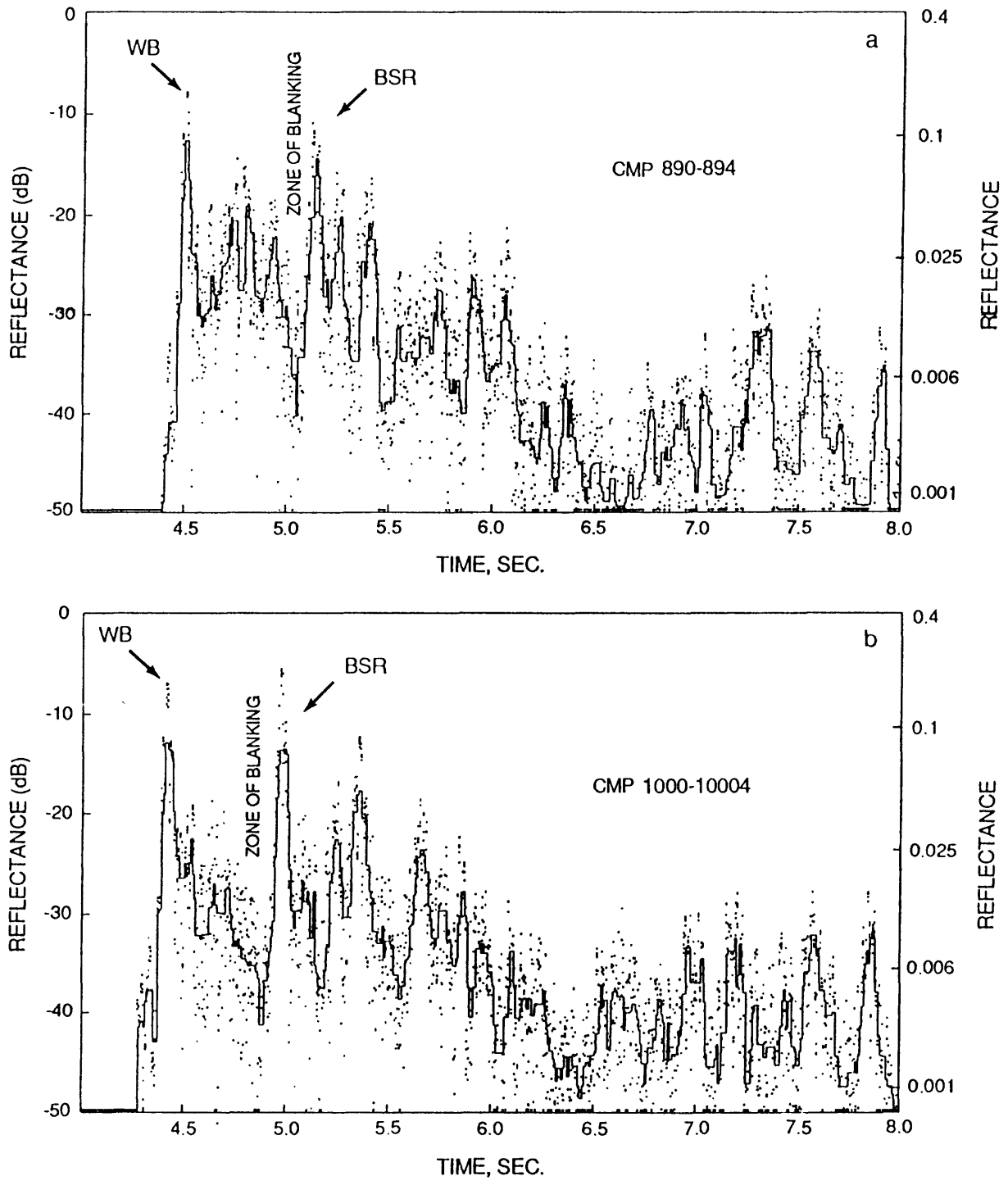

Figure 5. Graphs showing amplitude analysis for selected CMP groups of USGS line 32 (illustrated in Figure 3). Each dot represents the amplitude of an 8 ms window and the solid line represents a 5 point running median of 5 consecutive CMP's. WB stands for the water bottom. **a)** CMP 890 - 894 **b)** CMP 1000 - 1004

consecutive CMP's. The solid line is the 5 point median of the average amplitude of 5 consecutive CMP's. In other words, the solid line is the running average of reflection amplitudes over a moving window that is 32 ms in duration vertically by 5 CMP's horizontally. The dB scale was computed based on a reflection coefficient of 0.4, thus we can get the absolute value of the reflection coefficient (i.e., the reflectance) directly from the plot. Although the magnitude of reflectance varies with the degree of interference and frequency content on band-pass filtered seismic sections such as those used in this study, it is a useful quantity in comparing relative reflection strength between seismic lines or along the same line.

The velocity and amplitude analyses can be combined via inversion theory by estimating the detailed interval velocity based on seismic amplitude and phase (Lindseth, 1979; Cook and Schneider, 1983). Seismic inversion involves computing velocity values from seismic amplitude, assuming a constant bulk density for the subbottom sediments. Results from DSDP hole 533 showed that lithology and bulk density, where measured, changed little downhole between about 50 m and 400 m (Sheridan, Gradstein and others, 1983); hence the assumption of constant density is probably valid at least for the upper 400 m of the sub-sea-floor section. Because seismic data generally lack low frequency information, i.e., less than 5 Hz, the inversion method provides band-limited impedances, or velocities, from which only local velocity variations can be estimated. To get the absolute interval velocity values, the missing low-frequency component of velocity was provided by the detailed analysis of stacking velocity, as per the method of Lindseth (1979). The results of the inversion for USGS line 32 are given in Figure 6.

RESULTS

Velocity

The marked difference in elastic properties between gas hydrate and liquid water is the physical basis for our analysis of the acoustic properties of hydrated sediment. The acoustic properties of gas hydrate are similar to those of ice. The compressional velocity of naturally occurring biogenic (methane) gas hydrate is about 3.3 km/s (Sloan, 1990) and its density is about 0.9 g/cc, whereas the velocity of the interstitial water is about 1.5 km/s and the density is 1.0 g/cc. The compressional velocity of hydrate-bearing sediment is therefore higher than that of water-saturated sediment. Because the hydrate formation substantially increases the rigidity of the sediment, a more pronounced effect is expected on the shear wave velocity for hydrated sediment. However, little data exist for shear wave velocity in hydrate-bearing sediment. We thus restrict our analysis of interval velocities to estimates based on compressional-wave information.

The average interval velocities versus two-way traveltime through subbottom sediment at representative CMPs for 6 multichannel seismic lines we studied in the Blake Ridge area are shown in figure 4. In this plot, each letter denotes the average interval velocity between the sea floor and the BSR calculated for several CMPs from each line (A: TD2HI; B: TD2HG; C: BT-1; D: BT-8; E: Gilliss 2; H: USGS 32). For comparison, the average interval velocity versus subbottom depth, based on DSDP drilling results reported by Carson and others (1986), is indicated by the solid line; the dots indicate average interval velocities versus subbottom depth derived from refraction data along the western North Atlantic continental rise (Houtz, 1974). The average velocity measured by Houtz (1974) is higher than that determined by Carson and others (1986) for drill cores and is generally higher than the interval velocities estimated from the multichannel reflection data. The higher average velocity of the refraction data of Houtz (1974) probably reflects acoustic anisotropy of marine sediment, because most of the propagation path is parallel to the bedding planes. Our analysis uses the interval velocity based on the virtually vertically travelling waves of multichannel reflection returns.

Figure 4 shows that the average interval velocity in the Blake Ridge area is similar to that of

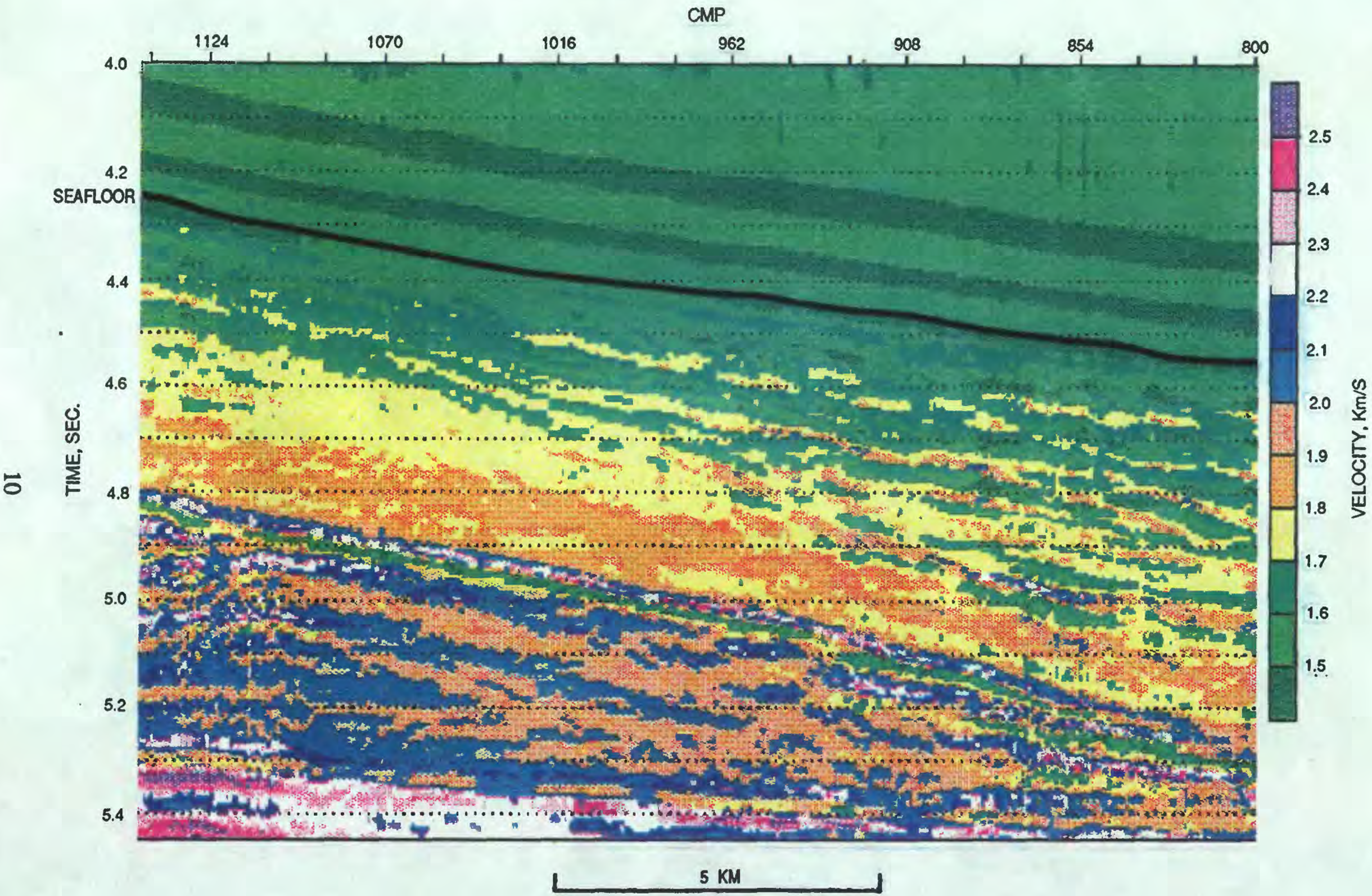

Figure 6. Detailed interval velocities created by the linear inversion of the data shown in Figure 3. The inversion was carried out using software by Hampson & Russell Software Service, Ltd.

marine sediment estimated by Carson and others (1986). In the Blake Ridge area, the BSR typically occurs near 600-ms two-way subbottom traveltime. If hydrates constitute a significant component of the sediment of the Blake Ridge, a noticeable increase of interval velocity would be anticipated in the sedimentary section above the BSR. However, we found no significant increase of average interval velocities on any of the seismic profiles. Possible explanations for this are:

1) The average concentration of gas hydrate in sediment is small, so the effect of gas hydrate on the seismic velocity measured by conventional stacking velocity analysis of multichannel seismic data may not be detectable. The gas hydrate could be finely disseminated throughout the sediment, and the change in bulk physical properties would thus be minimal.
2) The occurrence of hydrated sediment is highly localized in thin layers or as patches, so as not to affect significantly the average velocity of subbottom deposits.
3) The length of streamer or detector offset (on the order of 3.6 km) is not large enough to resolve small increases of interval velocity in deep water, in the range of 3 to 5 sec two-way traveltime (i.e., 2250-3750 m).
4) Localized differences in stratigraphy and lithology, data acquisition, and processing techniques might obscure true subbottom velocity relations. For example, the interval velocities for Gilliss 2 (letter E in Figure 4) is always less than the average curve by Carson and others (1986), whereas the interval velocities for USGS 32 (letter F in Figure 4) are mostly greater than the average velocity even though these two lines are near-by parallel seismic lines (fig. 1). This discrepancy could be partly due to the difference in field acquisition, that is, using a 1.2 km streamer for Gilliss 2 and a 3.6 km streamer for USGS 32.

So far, our analysis would suggest average interval velocities from multichannel data are not diagnostic in estimating hydrate concentrations in the Blake Ridge area.

Amplitude

Amplitude variations associated with the presence of gas hydrates are obvious in the Blake Outer Ridge area. Figure 3 shows, in color, the amplitude of reflected energy along part of USGS 32. A low amplitude, or blanking, zone is just above the BSR; the thickness of this zone of blanking varies spatially. Amplitude blanking above the BSR is common throughout the area and suggests that wherever a BSR is recorded, a corresponding amplitude blanking zone will be detected immediately above it. This statement does not imply that all blanking zones correspond to hydrated sediment.

Figure 5 reveals that the average seismic amplitude immediately above the BSR is small; the reflectance of this zone is less than 0.01. The zone of blanking is wider for CMP 1000-1004 (Figure 5b), than for CMP 890-894, in agreement with the seismic section shown in Figure 2. The blanking has a transitional character for CMP 1000-1004, but it is a sharp change for CMP 890-894. The average amplitude for the section between the water bottom and the BSR is about -30 dB, which is a reflectance of about 0.0125, for CMP 1000-1004 and about -24 dB (reflectance of 0.025) for CMP 890-894. If the amplitude blanking records the presence of gas hydrates, then Figures 3 and 5 suggest that a thicker zone of hydrated sediment occurs near CMP 1000 than near CMP 890. Also, the differences in reflectance may be related to the amount of hydrate present in the sediment.

Relation between velocity and amplitude

In order to assess the relation between amplitude blanking and interval velocity, a composite plot, shown in Figure 7, for the interval velocity derived from stacking velocities versus median reflectance for a window about 200 ms above the BSR was prepared. The points are scattered, but a general relation showing a decrease in amplitude with respect to an increase in velocity exists. The maximum amplitude variation for a given interval velocity is about 15 dB at an interval velocity of about 2000 m/s, and the interval velocity changes between 1700 m/s and ~ 2100 m/s for the median reflectance of 0.025 (about -13 dB point). The consistently low interval velocity for the Gilliss-2 data (letter E in Figure 7) probably reflects the short streamer offsets (1.2 km).

Many factors can contribute to the large scatter of interval velocity vs median reflectance. These factors include the following:

1) Localized changes in stratigraphy, lithology, and hydrate concentration. In the Blake Ridge region, these lateral variations are probably not large, but small variations could certainly contribute to the observed scatter.
2) Differences in the original frequency content of the source affect median reflectances.
3) A bulk bias in the reflection amplitude. This may exist for each line because of inaccurate water-depth corrections in the median reflectance calculations.
4) Difficulties in picking arrival times affect estimated interval velocity determinations.
5) Variable length of the time windows used in the velocity analysis, because there are no laterally continuous reflection events to guide picks.
6) Lack of resolution. Because of relatively deep water depths and low interval velocities of hemi-pelagic sediments, the employed streamer length is not sufficiently long to extract accurate interval velocity measurements from stacking velocities.

Factors 5 to 7 easily introduce 100 m/s velocity changes by slightly changing the reflection arrival times, resulting in large uncertainties in individual velocity estimations. The important observation from Figure 7 is that the average interval velocity of the section immediately above the BSR, which is presumably mostly hydrated sediment, varies between 1700 m/s to 2000 m/sec and the median reflectance varies between 0.05 and 0.01. This observation is fully utilized in building our working model for estimating the amount of gas hydrate in deep marine sediment.

A second method to compare velocity and reflection amplitude is through inverting the amplitude information for velocity, which is demonstrated for USGS line 32 in Figure 6. This plot clearly reveals that the high amplitude BSR reflection arises from the presence of a low-velocity layer (green color), an observation consistent with the presence of free gas trapped beneath the base of the hydrate stability zone which is delimited by the BSR (Dillon and Paull, 1983). In the section above the BSR, the region near CMP 890 shows a thicker low-velocity zone (green) than the region near CMP 1000-1100, implying that less hydrate exists near CMP 890 than CMP 1100. This result agrees qualitatively with the amplitude blanking (Figure 5) near CMP 890 that exhibits a smaller reflectance (i.e., less hydrate concentration) than that near CMP 1000 (i.e., more hydrate concentration).

Summary

Based on the analysis of 6 seismic profiles from the Blake Ridge area, we can make the following statements:

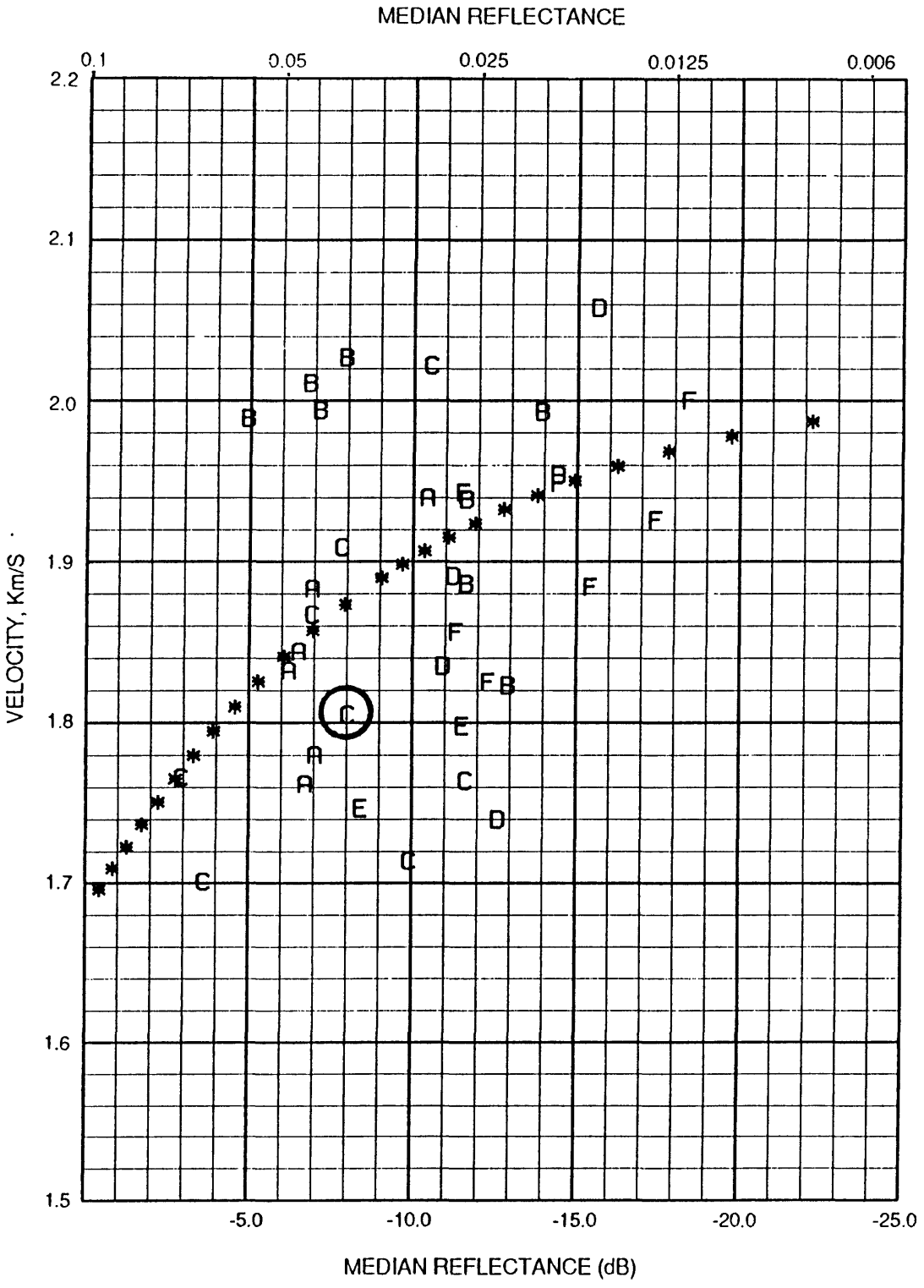

Figure 7. A graph showing relation between average interval velocities (from stacking velocities) estimated from a zone about 200 ms above the BSR downward to the BSR and median reflectance in this zone. Each letter represents values from CMPs on the six seismic profiles: A, B, C, D, E, and F represent TD2HI, TD2HG, BT1, BT8, Gilliss 2, and USGS 32, respectively. Asterisks (*) represent the theoretical relationship between velocity and relative median reflectance (or blanking) derived from Model 4. Point C is the velocity reflectance value closest to DSDP 533.

1) The amplitude of seismic reflections from within the hydrate stability zone is generally much lower in the area where there is an observed BSR. Thus, amplitude blanking may be a useful seismic attribute related to the presence of gas hydrate.
2) Based on stacking velocity data, the average interval velocities of subbottom sediment between the sea floor and the BSR are similar to the average interval velocity of non-hydrate bearing marine sediments. This observation implies that even though hydrated sediment occurs in the Blake Ridge area, the amount of gas hydrate may be small.
3) Although precise velocities are difficult to determine, the velocity structure derived by the inversion method displays a close correlation to the pattern of median reflectance (e.g., compare Figures 3 and 6). Thus, we believe that these parameters may be fundamentally related, and we propose to use seismic amplitude to estimate the amount of gas hydrate in the Blake Ridge area.
4) The interval velocity of the lower portion of the sediment varies between 1700 m/s and 2000 m/s and the median reflectance varies between 0.05 to 0.01.

PHYSICAL BASIS FOR MODELING HYDRATES

Currently, how the presence of gas hydrate affects seismic velocity of slope sediments is not known. Timur (1968) first proposed a three-phase time-average equation to explain the velocities of compressional waves in various consolidated rocks measured at permafrost (i.e., subzero) temperatures. Pearson and others (1983) applied the equation to hydrated rock and concluded that it qualitatively explains the known sonic properties of hydrated sediment in consolidated media. They used the following 3-phase, time-average equation for the velocity:

$$\frac{1}{V_p} = \frac{\phi(1-S)}{V_w} + \frac{\phi S}{V_h} + \frac{(1-\phi)}{V_m}, \qquad (1)$$

where
V_p : compressional velocity of the hydrated sediment
V_h : compressional velocity of the pure hydrate
V_w : compressional velocity of the fluid
V_m : compressional velocity of the matrix
ϕ : porosity (as a percent)
S : concentration of hydrate in the pore space (as a percent)

Several workers have demonstrated that the observed velocity behavior of some normal (i.e., unhydrated) rocks is not always consistent with the predictions of the time-average model. Four of the conditions causing discrepancies are: (1) if the rock is unconsolidated or lightly cemented (Wyllie and others, 1958); (2) if the rock contains a significant amount of organic material (Timur, 1968); (3) if the rock contains a significant amount of clay (Castagna and others, 1985; Eberhart-Phillips and others, 1989); and (4) if the rock contains secondary porosity, such as fractures (Wyllie and others, 1958).
The fourth condition pertains to crystalline or other consolidated rocks and is not relevant to most slope sediments. The first three conditions, however, apply to sediments found on the Blake Outer Ridge: they are unconsolidated, contain about 50% clays, and have organic carbon content that ranges from 0.5 to 1.4% (Sheridan, Gradstein and others, 1983; Kvenvolden and Barnard, 1983). To accommodate these discrepancies, some workers have applied correction factors to the time-average equation (e.g., Asquith and Gibson, 1982; Castagn and others., 1985).

The interval velocities computed from the time-average or modified time-average equations did not fit the observed interval velocities obtained from DSDP samples in the study area. We propose an equation of interval velocities for marine hydrated sediments using the approach of

Nobes and others (1986), who computed the interval velocities of marine sediments by a weighted mean of the time-average equation (Wyllie and others, 1956) and Wood equation (1941). The Wood equation is approximately valid for particles in suspension, and is defined as:

$$\frac{1}{\rho V^2} = \frac{\phi}{\rho_w V_w^2} + \frac{(1-\phi)}{\rho_m V_m^2} \tag{2}$$

where V : compressional velocity of sediments
ρ : bulk density of sediments
ρ_w : density of the fluid
ρ_m : density of the matrix

Like the 3-phase time-average equation, the Wood equation for hydrated sediments can be written as:

$$\frac{1}{\rho V^2} = \frac{\phi(1-S)}{\rho_w V_w^2} + \frac{\phi S}{\rho_h V_h^2} + \frac{(1-\phi)}{\rho_m V_m^2} \tag{3}$$

where ρ_h : density of the pure hydrate

The proposed equation for the interval velocity for hydrated deep marine sediment is a weighted mean of equations (1) and (3); that is,

$$\frac{1}{V_p} = \frac{W\phi(1-S)}{V_1} + \frac{1-W\phi(1-S)}{V_2} \tag{4}$$

where V_1 represents the Wood velocity, V_2 is the Wyllie velocity, and W is a weighting factor. When S=0, in the case that there is no hydrate, equation (4) is identical to the equation of Nobes and others (1986). As the porosity decreases, equation (4) approaches the 3-phase time-average equation of Pearson and others (1983).

The relationship between compressional velocity and porosity for unconsolidated sediments sampled by DSDP on the U.S. Atlantic continental rise (Table 1) is shown in Figure 8 together with theoretical curves of Wood (1941) and Wyllie and others (1956) and equation (4) with W=1 and S=0. The matrix velocity is set equal to the value of the velocity for zero porosity and 65% clay content, 4.37 km/s (Castagna and others, 1985).

In higher porosity ranges, equation (4) is close to the Wood equation, while at lower porosities, equation (4) is similar to the time-average equation. As indicated in Figure 8, the average equation (4) with W=1.0 fits the observed interval velocities quite well for porosities greater than about 40%. Thus, throughout our model study, we used W=1.0.

A knowledge of both velocity and density is required to understand and model reflections. To derive density, we can use the weighted average of constituent components. That is,

$$\rho_p = (1-\phi)\rho_m + (1-S)\phi\rho_w + S\phi\rho_h, \tag{5}$$

where ρ_p : bulk density of the hydrated sediment
ρ_h : density of the pure hydrate
ρ_w : density of the fluid
ρ_m : density of the matrix

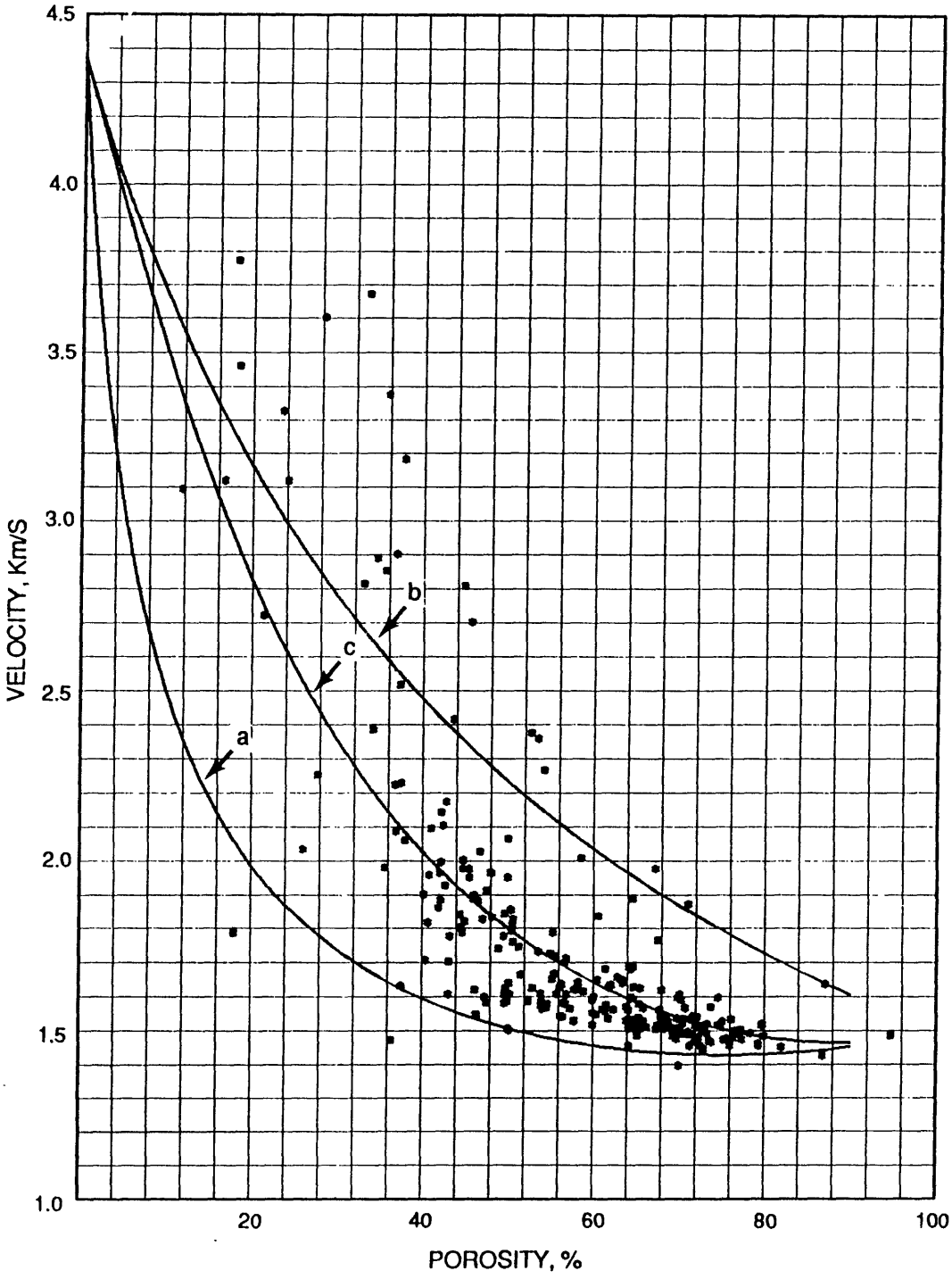

Figure 8. Graph showing observed velocity-porosity values (symbols) for sediment on the U.S. Atlantic continental rise from DSDP sites listed in Table 1 and predicted curves (solid lines) for velocity-porosity relations calculated using the Wood equation (curve a), time-average equation (curve b), and average equation (curve c) (The source of the porosity-velocity values is DSDP CD-ROM data set, NGDC-03, produced by NGDC with support from the U.S. Science Support Program of the Joint Oceanographic Institutions, Inc.).
a) Result of Wood equation using matrix velocity of 4.37 km/s.
b) Result of time-average equation using matrix velocity of 4.37 km/s.
c) Result of average equation we used in this study.

DSDP Hole	Latitude	Longitude
101	25.1988° N	74.4385° W
103	30.4513° N	75.5832° W
104	30.8725° N	74.3273° W
105	34.8953° N	69.1733° W
384	40.3608° N	51.6633° W
385	37.3695° N	60.1575° W
390	30.1423° N	76.1123° W
390a	30.1423° N	76.1123° W
391a	28.2268° N	75.6167° W
391c	28.2268° N	75.6167° W
417a	25.1105° N	68.0413° W
418a	25.0350° N	68.0573° W
418b	25.0347° N	68.0575° W

Table 1.-- The location of DSDP holes on the Atlantic continental rise. The compressional velocity and porosity sampled by these DSDP holes were used in this analysis

MODELS

If amplitude blanking is a seismic attribute related to gas hydrate cementation in slope sediment, can the relation between interval velocity, reflection amplitude, and hydrate cementation be established? In order to answer this question, we investigated simple one-dimensional models. Our objective is to construct a model in which amplitude blanking increases as interval velocity (and therefore hydrate concentration) increases, in accordance with the observations presented earlier. Significant blanking must also occur at relatively low interval velocities.

For the first three models, we assume that hydrate forms only in the pore spaces of the sediment, i.e., 0% hydrate means no hydrate exists in the pores; 50% hydrate means 50% of the pore space is filled by hydrate; and 100% hydrate means all of the available pore space is filled by hydrate. We then define a geologic boundary (i.e., reflecting horizon) across which porosity or lithology (or both) changes. The velocity of the sediment on either side of the boundary can be calculated for all values of hydrate concentration (0-100%) using the average equation (equation 4). The density of the sediment can be derived using the weighted proportions of the constituent components (equation 5). Typical values for parameters in the average equation are given in Table 2. From the velocity and density values, the normal incidence reflection coefficient at the boundary **without** hydrate cementation is:

$$R = \frac{\rho_2 V_2 - \rho_1 V_1}{\rho_1 V_1 + \rho_2 V_2}, \tag{6}$$

where R is the reflection coefficient; subscript 1 indicates the upper medium, and subscript 2 indicates the lower medium. Likewise, the reflection coefficient across the boundary **with** hydrate cementation is:

ρ_m = 2.7, 2.72 g/cc	(matrix density)
ρ_h = 0.9 g/cc	(hydrate density)
ρ_w = 1.0 g/cc	(water density)
V_m = 4.47, 4.8 km/s	(matrix velocity)
V_h = 3.3 km/s	(velocity of pure hydrate)
V_w = 1.5 km/s	(velocity of water)
ϕ = 45 - 62.5 %	(porosity)

* The values of ρ_m and V_m vary as specified in the text.

Table 2.-- Physical property values used in the model study*

$$R_h = \frac{\rho_2' V_2' - \rho_1' V_1'}{\rho_2' V_2' + \rho_1' V_1'}, \tag{7}$$

where R_h and the prime indicates the properties of the sediment containing hydrate.

The amplitude ratio γ, which is a measure of the amount of blanking, is therefore:

$$\gamma = \frac{R_h}{R} \tag{8}$$

The best fit model is one in which γ decreases from 1 to some small value as interval velocity and hydrate concentration increase.

A) Model 1--both porosity and hydration boundary

This model causes a reflection to occur at a boundary that is both a porosity and hydrate discontinuity. Figure 9 shows the velocity, density, and blanking factor with respect to the hydrate concentration with

$$\phi_1 = 50\%, \phi_2 = 45\%, V_m = 4.37 \text{ km/s, and } \rho_m = 2.7 \text{ g/cc}$$

and other parameters given in Table 2. This figure illustrates an amplitude decrease (blanking) that is proportional to the hydrate concentration (dashed curve in figure 9), but the amplitude loss is very small. For example, at 100% filling of the pore space by hydrate, which indicates 50% hydrate in the sediment of the upper medium and 45% hydrate in the lower medium, the amplitude ratio is still greater than 0.5. The interval velocity at 100% saturation approaches about 3.8 km/s and densities are decreasing with increasing concentration because of the hydrate's low density. This model predicts a small amount of blanking, which is quite different from what we observe in figure 7.

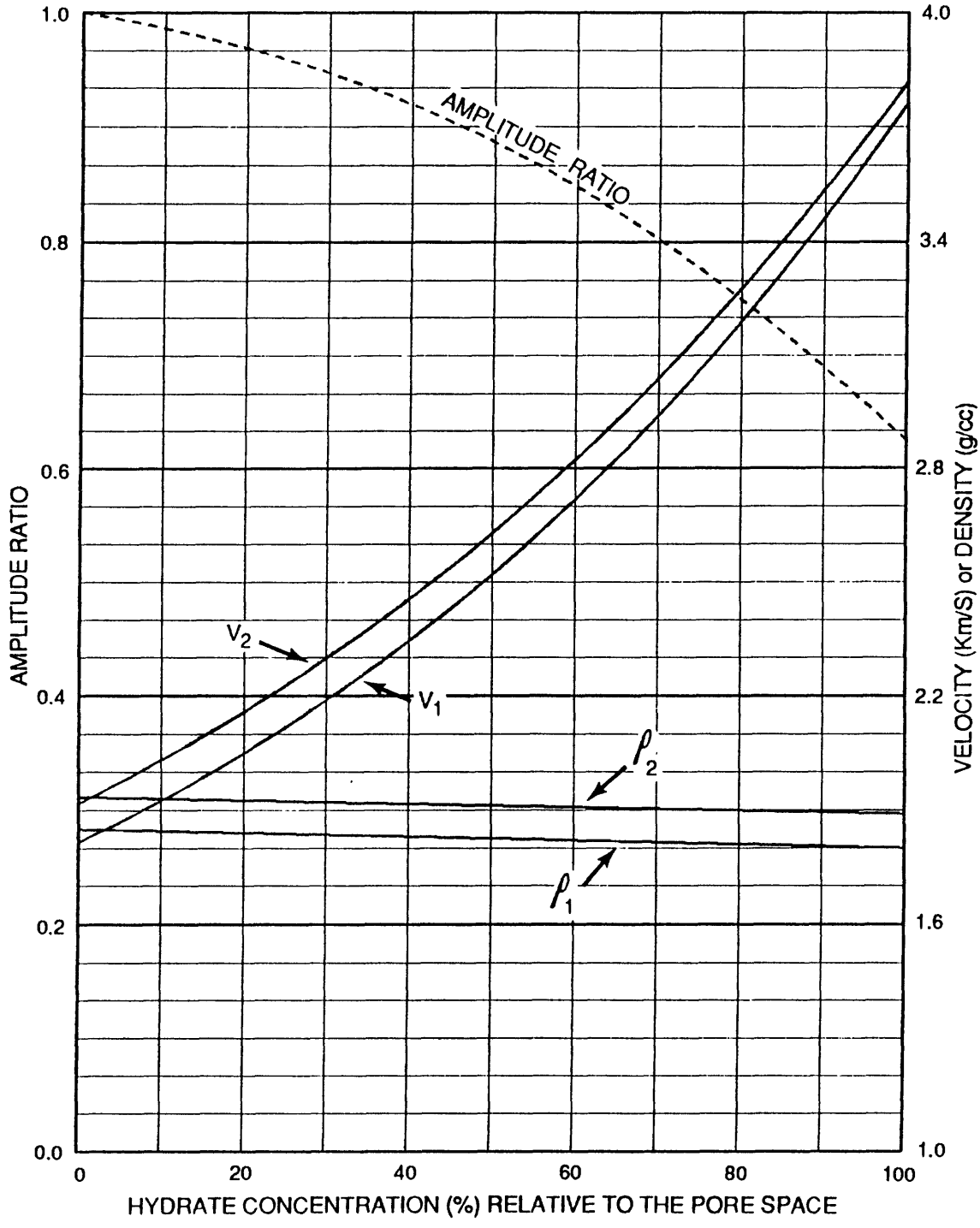

Figure 9. Model 1: Computedvelocity and density (solid lines) and amplitude decrease, or blanking (dashed line), relative to the proportion (i.e., percent) of gas hydrate filling the pore spaces of sediment above and below a reflecting interface that is defined as a porosity boundary. *V* and ρ denote compressional velocity and density respectively and subscripts 1 and 2 indicate the upper medium and lower medium, respectively (ϕ = 50%, ϕ = 45%). In this model, the amount of hydrate above and below the interface varies directly with porosity.

B) Model 2--porosity boundary and constant hydration

Model 2 is similar to model 1 in causing a reflection to occur at a porosity boundary with ϕ_2 = 60% and ϕ_1 = 50%, but in this model, we assume that the amount of hydrate is constant across the boundary. The result of this model indicates a decrease of amplitude at the reflection boundary, but the rate is much slower than that of model 1.

C) Model 3--porosity and lithological boundary

This model assumes that a reflection occurs at a lithologic boundary characterized by a change in both matrix velocity, matrix density, and porosity. We assume that hydrate concentration is proportional to the porosity across the boundary. The justification for using different matrix velocities can be understood by considering the difference of clay content in marine sediments. In this model the lower medium has less clay content than the upper-medium. We use the following acoustic properties for this model:

For Upper Medium	**For Lower Medium**
V_{m1} = 4.37 km/s	V_{m2} = 4.8 km/s
ρ_{m1} = 2.7 g/cc	ρ_{m2} = 2.73 g/cc
ϕ_1 = 60 %	ϕ_2 = 50 %

Similar to the result of model 1, model 3 predicts an amplitude decrease with respect to increasing hydrate concentration, but the amplitude blanking is too small compared to our observation. For example, at 100% concentration of hydrate, the amplitude ratio is only 0.87.

If we interchange the porosity values of model 3, that is, ϕ_1 = 50% and ϕ_2 = 60%, there is higher amplitude blanking. However, the amount of blanking is still less than our observation. For example, at 100% concentration, the amplitude ratio is about 0.55.

Each of the three models we described is feasible in terms of hydrate cementation processes, but none predicts a high amplitude decrease as interval velocity increases.

D) Model 4--Sediment substitution

In order to account for the observed high amplitude blanking with low interval velocities, we introduce an alternative model. This model involves the mixing of two end members; one consisting of marine sediment devoid of gas hydrate and the other consisting of a "representative hydrated sediment". The model we adopt is that the observable seismic characteristics of gas-hydrate sediment can be explained by the replacement or substitution of unhydrated marine sediment by the "representative hydrated sediment" across the reflecting boundary. The important difference between this model and models 1-3 is that, as the hydrated end member replaces the unhydrated end member, the reflecting boundary disappears at 100% replacement and only "representative hydrated sediment" occurs.

The representative hydrated sediment consists of a 57.5% porous sediment that contains gas hydrate in only 27.5% of the pore space. To illustrate the blanking effect by model 4, we can use any kind of "representative hydrated sediment". We choose an average 57.5% porosity because this is what we get by solving the regression equation (4) for porosity using the lowest observed velocity (about 1700 m/s from figure 7). The lowest measured velocity represents the best estimate for unhydrated sediment. A porosity of about 60% was also measured in three samples from DSDP 533 and therefore porosity of 57.5% seems appropriate for the Blake Ridge area. We get 27.5%

concentration of hydrate in the pore space by solving equation (4) for S (hydrate concentration) using ϕ = 57.5% (porosity) and $V_p \approx$ 2000 m/s (compressional velocity of hydrated sediment), which was taken as the highest average velocity for hydrated sediment in the Blake Ridge area (fig. 7). If we had used V_p = 2100 m/s, the hydrate concentration would be 34%. We preferred to use the lower, more conservative estimate. The uncertainty in hydrate concentration could be as high as 25% in this example.

The velocity (V_{hs}) and density (ρ_{hs}) of the representative hydrated sediment in the model are from equations (4) and (5) with the acoustic parameters for model 1: V_{hs} = 2.016 g/cc, ρ_{hs} = 1.707 g/cc. The acoustic properties of the unhydrated sediment are: V_1 = 1.625 km/s, ρ_1 = 1.638 g/cc, ϕ_1 = 62.5%, V_2 = 1.768 km/s, ρ_2 = 1.808 g/cc, ϕ_2 = 52.5%

Figure 10 illustrates the seismic amplitude versus the percent substitution of "representative hydrate sediment", i.e., 0% representative hydrated sediment refers to no hydrate present; 40% refers to the substitution of 40% representative hydrated sediment into both the upper and lower media; and 100% refers to complete replacement of the upper and lower media by representative hydrated sediment. It is clear from Figure 10 that the amplitude blanking is proportional to the amount of the representative hydrated sediment, and the amount of hydrate in the sediment is a single function of the amplitude blanking. At the 100% point, the amplitude ratio is 0 (which is a total blanking), because all unhydrated sediment is replaced by the representative hydrated sediment. The highest velocity in this model is 2.02 km/s, which is the compressional velocity of the representative hydrated sediment. This model predicts significant blanking with a low interval velocity.

We can redisplay the results of Figure 10 in terms of relative median reflectance and interval velocity, and this is shown as stars (*) in Figure 7. This predicted curve is consistent with the observations in as much as it falls within the scatter of the data and the maximum and minimum reflectance and velocity values coincide with the maximum and minimum observed values.

Two independent lines of evidence support the validity of the results of model 4. First, we used velocity information (Figure 7) to calculate a porosity of 57.5% for the model (equation 4). This value is essentially identical to that measured in DSDP 533 in an interval near the bottom of the hole (Sheridan, Gradstein, and others, 1983). Second, point C, which is circled in Figure 7, is less than the 100 m/s away from the modeled curve which is well within the accuracy of the velocity pick. This point is the reflectance/velocity value from line BT 1 closest to DSDP 533, which is the only place in the study area where the model can be realistically calibrated.

BULK VOLUME OF GAS HYDRATE

Our goal in modelling amplitude blanking is to develop a method for estimating the amount of gas hydrate in marine sediment from attributes (i.e., velocity and amplitude) contained in seismic reflection data. Models 1-4 suggest some of the mechanisms by which blanking might occur, but only model 4 predicts significant blanking at low interval velocities (around 2 km/s). Model 4 is therefore our choice for estimating the total amount of gas hydrate in the Blake Ridge sedimentary column. In this section, we describe some of the uncertainties in estimating bulk volume of gas hydrate in sediment by analyzing a family of models related to model 4. Our results show how amplitude blanking, if calibrated by velocity information, can be used to estimate the bulk volume of gas hydrate in sediment. This approach provides a technique that might be used with single channel data, which do not contain velocity information, but which are widely available over the world's oceans.

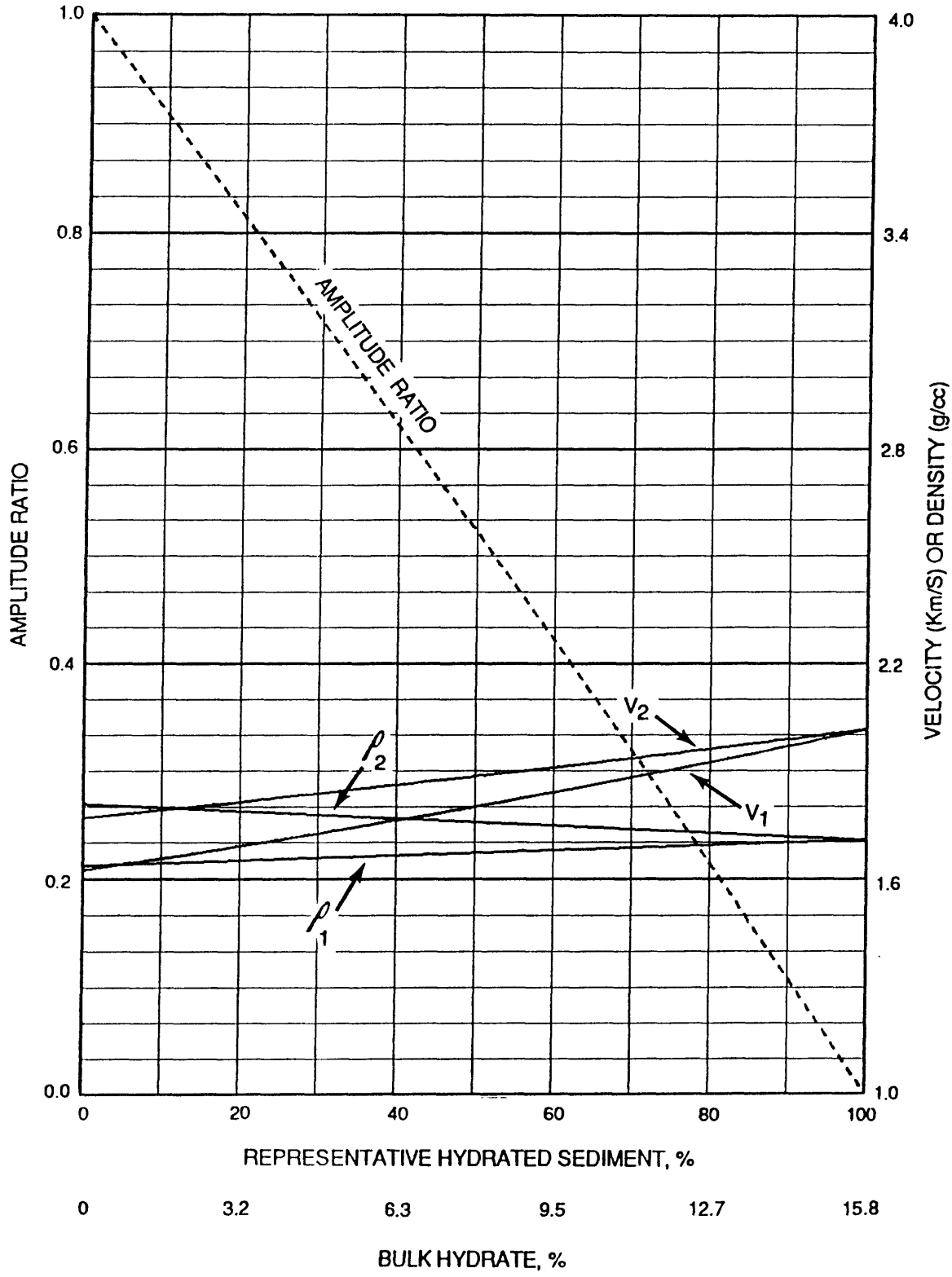

Figure 10. Model 4: Computed velocity and density (solid lines) and amplitude decrease (dashed line) relative to the proportion of representative hydrated sediment (57.5% porosity rock with 27.5% of the pore space filled by gas hydrate) that replaces unhydrated marine sediment across a porosity boundary. V and ρ denote compressional velocity and density respectively ($\phi_1 = 62.5\%, \phi_2 = 52.5\%$). In this example, the amount of hydrate is identical above and below the reflecting interface and is equal to the proportion of hydrate contained in the representative hydrated sediment that is mixing with/replacing the unhydrated sediment.

When only amplitude information is used to estimate hydrate concentration, some uncertainties exist, mainly because changes in amplitude are a secondary effect of the hydrate cementation. Amplitude only measures relative changes in acoustic impedences. Some of these uncertainties can be clarified using the graph shown in Figure 11, which shows amplitude blanking for five different cases of "representative hydrated sediment" that is substituted in equal proportions above and below a reflecting interface. Curves **a** to **e** in Figure 11 use the same initial parameters as model 5, except that gas hydrate fills the pore spaces by 20%, 40%, 60%, 80%, and 100% respectively. The amplitude blanking curve of model 4 (27.5% gas hydrate in the pores; Figure 10) would be intermediate between curves **a** (20%) and **b** (40%). Five average velocity curves are also plotted, in which average velocity is the average of the upper- and lower-medium velocities.

This graph can be used to calculate the bulk volume of gas hydrate in the sediment. For example, curve **b** shows the amplitude blanking for representative hydrated sediment in which 40% of the 57.5% pore volume is filled with hydrate, i.e., the maximum bulk volume of gas hydrate is 23% (40% of 57.5%). The horizontal axis gives the percent of this representative hydrated sediment that is substituted above and below the reflecting interface. At a value of 50% substitution, the bulk volume of gas hydrate is 11.5% (50% of 23%). The value of the amplitude ratio for curve **b** at 50% substitution can be read directly from Figure 11 and is about .53 times the amplitude of the reflection that occurs with no gas hydrate in the pore spaces.

The five amplitude-ratio curves in Figure 11 are similar to each other despite large differences in the velocity of the hydrated sediment. Amplitude blanking is slightly higher for lower concentrations of hydrate, but the difference between high and low concentration is negligible for our purpose. This small difference suggests that estimates of the percent of representative hydrated sediment within the blanking zone are robust, although the concentration of hydrate within the pore spaces remains uncertain. This uncertainty in the amount of hydrate filling the pore volume obviously affects estimates of the bulk volume of hydrate in the sediment.

For example, suppose we measure a blanking of 0.5. Let us use the representative hydrated sediment "a", which is 20% hydrate concentration in 57.5% porosity rock, for our estimation. The position where curve **a** has an amplitude ratio of 0.5 corresponds to substitution of representative hydrated sediment by 50%. Thus, the bulk volume of hydrate in the sediment is about 6%, (i.e., 0.575 x 0.2 x 0.52 ≈0.06). Values of bulk volume for curves **b**, **c**, **d**, and **e** are 12%, 19%, 26%, and 33% respectively. Curve **e** yields a value about 5 times larger than curve **a**. This illustrates that for a given reflectance or blanking, there is a large difference in the estimates of bulk volume of gas hydrate.

If interval velocity is used to determine estimates of bulk volume of hydrate, a small range of values is obtained. For example, suppose that the interval velocity of hydrated sediment is 2 km/s. The concentrations of representative hydrated sediment corresponding to 2 km/s (Figure 14) are .65 for curve **b**, .44 for curve **c**, .33 for curve **d**, and .27 for curve **e**. Curve **a** never reaches an average velocity of 2 km/s. Bulk volume estimates are 15% hydrate for curve **b** (.575 x .4 x .65), 15% for curve **c**, 15% for curve **d**, and 16% for curve **e**. This scatter of 1% (15-16%) is negligible.

If interval velocity can be combined with amplitude blanking information, then a reasoned choice of curves **a-e** become possible. Suppose the observed interval velocity is 2 km/s and the observed amplitude blanking is 0.5. The bulk volume of gas hydrate from interval velocity determination is 15-16%, as calculated above. From our earlier example of amplitude blanking equal to 0.5, curve **c** offers the closest comparable estimate (19% bulk volume). In this hypothetical case, the interval velocity calibrates the amplitude-blanking calculation and provides the basis for choosing curve **c** (60% hydrate concentration in the pore spaces) as the best fit.

A better example is provided by examining the reflectance and velocity information from the point closest to DSDP 533 (point **c** circled in Figure 7). This has an average interval velocity of 1800 m/s, and a reflectance of 0.042 which corresponds to an amplitude blanking of about 0.5. If

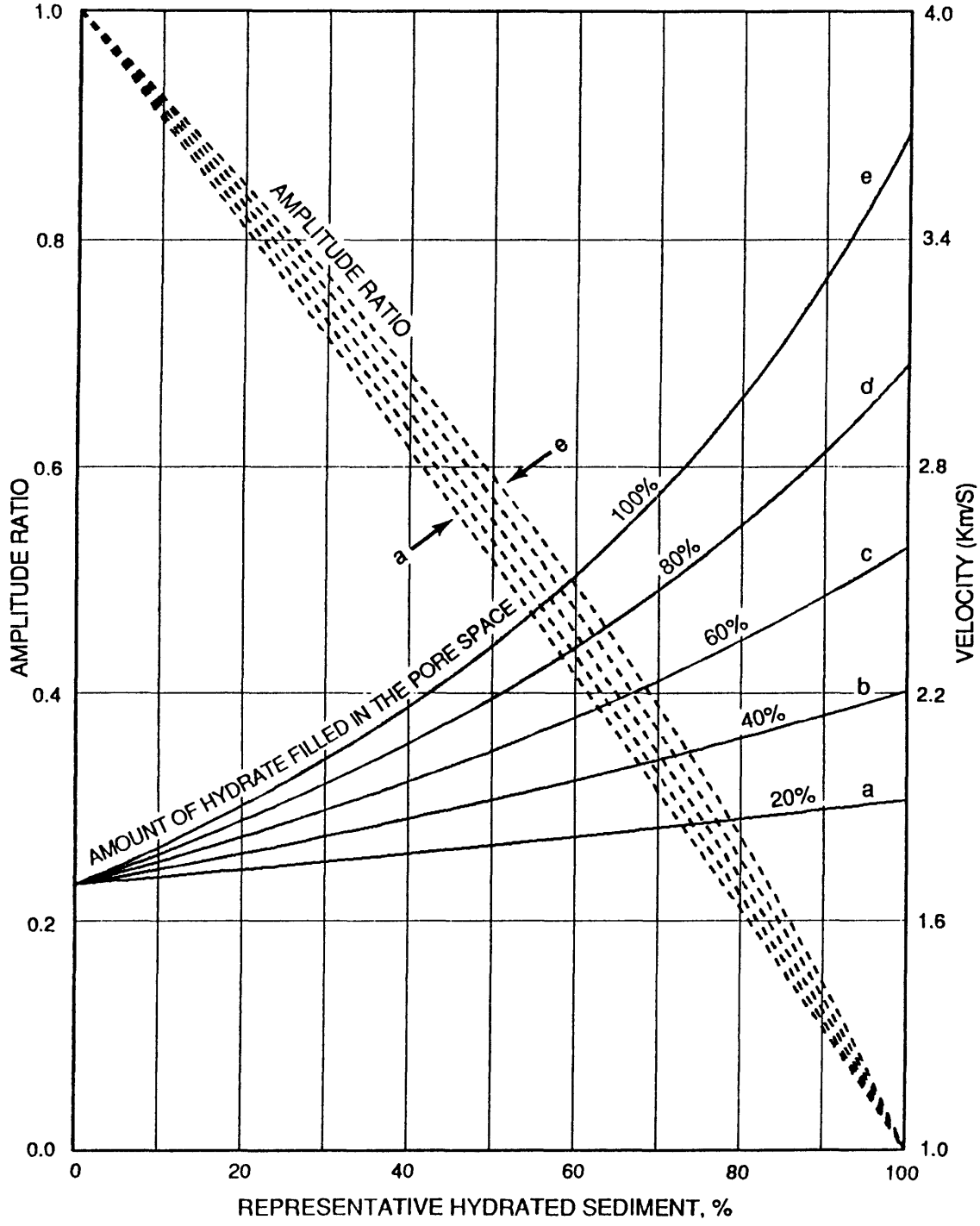

Figure 11. Average interval velocities (solid lines) and amplitude blanking curves (dashed lines) across a porosity boundary resulting from replacing unhydrated marine sediment by representative hydrated sediment. Each of the five representative hydrated sediment cases used in the graph (curves **a-e**) consist of rocks having 57.5% porosity with the following concentrations of hydrate in the pore spaces: **a** - 20%; **b** - 40 %; **c** - 60%; **d** - 80%; **e** - 100%. Model 4 (Figure 10) shows the case where the concentration of the hydrate in the pore spaces is 27.5%.

bulk volume is calculated from model 4 (Figure 10), the value based on amplitude blanking is about 9.5%, and the value based on an average velocity of 1800 m/s (the midpoint between the points where curves V_1 and V_2 cross the 1800 m/s value) is about 6% in total volume. At site 533, methane gas was sampled and presumed to indicate the existence of disassociated gas hydrate. A single measurement yielded 13 volumes of gas to 1 volume of sediment (Kvenvolden and Barnhard, 1983). Because gas hydrate concentrates methane in the ratio of about 160:1 (Kvenvolden, 1988), the resulting value for the bulk volume of gas hydrate in the sediment is 13:160, or about 8%, which agrees with the 6-9.5% prediction from model 4. Whether 8% is a maximum or only average concentration remains uncertain, because it is the only measurement available from site 533.

In summary, the amplitude information yields robust estimates of the percent of representative hydrated sediment substituted above and below a reflecting horizon, but cannot constrain the concentration of gas hydrate in the pore spaces. Hence amplitude information alone produces large uncertainties in the bulk volume of hydrate in the sediment. Interval velocity, however, yields a small range of values for bulk volume of gas hydrate regardless of the large differences in percent of representative hydrated sediment. Calibrating the bulk volume of hydrate deduced from amplitude information with the bulk volume calculated from velocity information provides the critical step in determining the appropriate concentration of hydrate in the pore space to be used in the model.

DISCUSSION

We have proposed a model for quantitatively estimating the bulk volume of gas hydrate in the zone above the BSR. The model (model 4) relates amplitude blanking, seismic velocity, concentration of gas hydrate in the pore spaces, and the concentration of representative hydrated sediment above and below a reflecting interface. Our results are consistent with the amplitude blanking and average interval velocities measured in the Blake Ridge area from multichannel seismic data and with the observation that a small amount of gas hydrate occurs at DSDP 533. This method, therefore, provides a technique for classifying and mapping hydrate concentrations using a grid of seismic reflection profiles. Estimates of the volume of hydrate (or methane) contained within the sediments above the BSR can be made from the hydrate concentrations. Preliminary estimates in the Blake Ridge area is 66 x 10^6 m^3 of hydrate, or approximately 370 TCF of gas per one square km beneath the sea floor (Dillon and others, 1991). A separate technique exists for placing limits on the thickness of the free-gas zone beneath the hydrate (Miller and others, 1991). Together, these methods offer the first quantitative approaches to estimating the total amount of hydrate and gas locked in the shallow subbottom ocean sediment.

A troublesome aspect of our modeling exercise is that the models based on the physical principle of hydrate filling intergranular pore-space (Models 1 to 3) fail to explain the basic observation in the Blake Ridge that large blanking is associated with relatively low interval velocities. A couple of implications of this observation are:

(1) The average equation (equation 4) that relates the physical properties of the sediment and the hydrate is incorrect. Although it is beyond the scope of this paper to evaluate this possibility, other studies have supported the general validity of the time-average equation (equation 1) for gas hydrates in consolidated sediments (e.g., Pearson and others, 1983).

(2) Our supposition that hydrates nucleate and fill pore spaces is over-simplified. One mechanism for hydrate formation in sediments is that growth proceeds from disseminated to massive occurrences; another mechanism is that hydrates grow by recrystallization and annealng during pressure and temperature changes that accompany glaciation and eustacy (Sloan, 1990). To what extent physical or chemical processes control hydrate occurrence in sediments is a major unsolved problem in understanding clathrates and warrants additional study.

(3) Our one-dimensional seismic modeling is too simple to explain the observations. For example, the models assume second order boundaries for reflection interfaces, but the real boundaries may well be transitional. Since the reflection characteristics of a transitional layer (Justice and Zuba, 1986), are quite different from reflections of simple boundaries, additional amplitude decrease can happen. We also assumed that whole layers are uniformly cemented by gas hydrate, but the cementation can vary spatially. Thus, three-dimensional modeling including scattering provides better approximation of reflection amplitude of hydrated sediments.

Our preferred model, Model 4, is unsatisfying in that sediment substitution probably does not occur in nature. However, almost nothing is known about the details of natural occurrence of gas hydrates--how they are distributed in the pores, how they cement the grains, whether they are disseminated or concentrated in veins and nodules, et cetera. We present this model because it is the only description that fits our current understanding about hydrates in deep-marine sediments. The fact that we do not know what the model means simply opens new directions for research in the physical and chemical occurrence of hydrates in sediments.

Even though this model cannot be fully explained in terms of reflection seismology, our estimation method is based on the physics of hydrated sediments: that is, the hydrate cementation in the pore space increases the interval velocity of marine sediment. Since our estimation method uses seismic amplitude firmly constrained by the observed interval velocities, the proposed method is valid and accurate as far as the amount of hydrate is concerned.

Our preferred model can be applied to reflection data sets in other regions as long as certain conditions are met. First, processing of the reflection data must preserve relative amplitudes, these amplitudes must be calibrated relative to the reflection coefficient of the sea floor, and must be corrected for any water-depth dependence of the reflection coefficient. Amplitude preservation and calibration are inherently more difficult on single channel data from deep water where the first multiple or other information for computing the reflection coefficient may be lacking.

Second, velocity estimates from the region of interest are required. The average lowest velocity of sediment is used to calculate porosity (equation 4), and the average highest velocity of hydrated sediment is used with porosity, to calculate the hydrate concentration.

Third, amplitudes must be scaled to a reference reflectance. The median reflectance for the data from the Blake Ridge is estimated as 0.1 (Figure 7) and the dB scale is based on this reference reflectance. This reference reflectance was chosen after all reflection profiles were examined. It is a function of both the locality of the seismic profiles and the data processing procedure. The choice of reference reflectance is subjective, but as long as a reasonable value is chosen, estimates of the amount of hydrate will not be affected. The reference reflectance is important for comparing amplitudes among different geographic locations and different seismic acquisition/processing methods.

Fourth, the source of hydrate should be known. Most methane in hydrates is biogenic, formed by bacterial action at low temperatures, but some hydrate is thermogenic, formed by relatively high temperatures, and contains gases such as ethane and propane (Sloan, 1990). The estimated compressional velocity of pure biogenic hydrate is 3.3 km/s, whereas that of pure thermogenic hydrate is 3.8 km/s (Pandit and King, 1983). This difference will affect hydrate concentrations estimated in equation (4).

Fifth, different geologic regions will almost certainly require different "representative" hydrated sediment to be input to the model. We offer here a method for selecting a "representative" hydrated sediment using the observations from Figure 7: Use the velocity of unhydrated sediment as the velocity near the 0 dB or 0.1 reference reflectance line. For the Blake Ridge in Figure 7, this velocity is 1700 m/s. Estimate the average porosity of the ordinary marine sediment using this velocity (1700 m/s) and the equation (4). The average porosity for the hydrate zone can also be taken from drill hole data. For the Blake Ridge, both methods yield a porosity of 60%. Estimate the highest velocity for the hydrated sediment in the area. We used a conservative estimate of 2000 m/s (Figure 7). Calculate the amount of hydrate concentration by substituting this upper velocity

value and the estimated porosity into equation (4). For the Blake Ridge, we calculate that the concentration of gas hydrate in the pore spaces is 27.5%. Hence the representative hydrated sediment in the Blake Ridge contains 57.5% pore volume, and 27.5% of the pore space is occupied by gas hydrate.

CONCLUSIONS

The primary effect of hydrate cementation on the acoustic properties of marine sediment is an increase in interval velocity, and the quantitative analysis of interval velocity can be used to estimate the bulk volume of in situ gas hydrate. However, this approach is not practical in the Blake Ridge area because of large scatter and uncertainty in velocity estimates based on available multichannel reflection profiles.

Another seismic attribute of hydrate cementation is amplitude blanking. This phenomena is observed in single-channel as well as multichannel seismic profiles. Our model assumes that the degree of amplitude blanking is related to the amount of gas hydrate filling the pore spaces of the sediment.

We propose a method of estimating the amount of in situ gas hydrate in deep marine sediment using amplitude information above the BSR. Because amplitude blanking is a relative quantity, the estimation method must be calibrated against interval velocities. This method is based on measuring the degree of blanking in seismic models generated by the bulk mixture of sediment consisting of two end members, "representative" hydrated sediment and similar deposits having no hydrate. The properties of the representative hydrated sediment can be calculated from interval velocity information and the weighted equation of the time-average and the Wood velocities. Seismic amplitudes can then be directly computed and related to the bulk volume of gas hydrate in the sediment. The mechanism by which blanking occurs remains unexplained. The models which simply fill pore spaces with hydrate underestimate the amount of blanking. Our preferred model (model 4, sediment substitution) is difficult to reconcile with known natural processes. This emphasizes the need for research in how the physical and chemical presence of hydrates in sediments alters the bulk properties of those sediments.

In the Blake Ridge area, the end members of the best fitting model are a representative hydrated sediment consisting of sediment with 57.5% porosity in which 27.5% of the pore spaces are filled by gas hydrate and an unhydrated sediment with an average porosity of 57.5%. This method can be applied to other areas by selecting two reasonable end member sediments. We emphasize that the observed amplitude must be carefully calibrated by interval velocities.

ACKNOWLEDGMENTS

The authors would like to thank David Scholl and Michael Max for very helpful and numerous comments on the earlier version of the manuscript. We thank T. Shipley and T. Brocher for very constructive comments and suggestions. This work was funded by the Department of Energy and U.S. Geological Survey.

REFERENCES

Asquith, G., and Gibson, C., 1982, Basic well log analysis for geologists: Am. Assoc. Petrol. Geol. Methods in Exploration Series, Tulsa, Oklahoma, 216 p.

Carson, R.L., Gangi, A.F., and Snow, K.R., 1986, Empirical reflection travel time versus depth and velocity versus depth functions for the deep-sea sediment column: Journal of Geophysical Research, v. 91, p. 8249-8266.

Castagna, J.P., Batzle, M.L., and Eastwood, R.L., 1985, Relationship between compressional-wave and shear-wave velocities in clastic silicate rocks: Geophysics, v. 50, p. 571-581.

Cook, D.A., and Schneider, W.A. ,1983, Generalized linear inversion of reflection seismic data: Geophysics, v. 48, p. 665-676.

Dillon, W.P., Booth, J.S., Paull, C.K., Fehlhaber, K., Hutchinson, D.R., and Swift, B.A. ,in press, Mapping sub-seafloor resrvoirs of a greenhouse gas: Methane Hydrates: Marine Technology Society Transactions of the International Symposium on marine positioning.

Dillon, W.P., Fehlhaber, K., Lee, M.W., Booth, J.S., and Paull, C.K. ,1991, Methane hydrate in sea floor sediments off the southeastern U.S.: Amount and implication for climate change, NE/SE Geological Society of America meeting, Baltimore, March 14-16, 1991, 1991 Abstracts with Programs, p. 22.

Dillon, W.P., and Paull, C.K., 1983, Marine gas hydrate-II: Geophysical evidence, in Cox, J.L, ed., Natural gas hydrates: properties, occurrence and recovery, Butterworth Publishers, Boston, p. 73-90.

Dillon, W.P., and Popenoe, P., 1988, The Blake Plateau basin and Carolina trough, in Sheridan R.B. and Grow, J.A., eds., The Atlantic Continental Margin: U.S.: DNAG Geolgy of North America I-2, p. 19-55.

Dobrynin, V.M., Korotajev, Yu. P., and Plyuschev, D.V., 1981, Gas Hydrate: a possible energy source, in Mayer, R.G. and Olson, J.C., eds., Long term energy resources, Pitman, Boston, p.727-729.

Dragoset, B., Hargreaves, N., and Larner, K., 1987, Air-gun source instabilities: Geophysics, v. 52, p. 1229-1251.

Eberhart-Phillips, D., Han, D.H., and Zoback, M.D., 1989, Empirical relationships among seismic velocity, effective pressure, porosity, and clay content: Geophysics, v. 54, p. 82-89.

Ewing, J.I., and Hollister, C.H., 1972, Regional aspects of deep sea drilling in the western North Atlantic: Initial report of the deep sea drilling project 11, p. 951-973.

Gray, W.C., 1979, Variable norm deconvolution: Stanford Univ. Ph.D.Thesis, Palo Alto, California.

Houtz, R., 1974, Preliminary study of global sediments sound velocities from sonobuoy data, in Hampton, L., ed., Physics of sound in marine sediments, Plenum Press, New York, p. 519 - 535.

Justice, H.J., and Zuba, C., 1986, Transition zone reflections and permafrost analysis: Geophysics, v. 51, p. 1075-1086.

Kvenvolden, K.A., 1988, Methane hydrate - A major reservoir of Carbon in the Shallow Geosphere: Chemical Geology, v. 71, p. 41-71.

Kvenvolden, K.A., and Barnard, L.A., 1983, Gas hydrates of the Blake Ridge, Site 533: Deep Sea Drilling Project Leg 76, Initial report of the deep sea drilling project 76, p. 353-365.

Lashof, D.A., and Ahuja, D.R., 1990, Relative contributions of greenhouse gas emissions to global warming: Nature, v. 344, p. 529-531.

Lee,M.W., and Hutchinson, D.R., 1990, True-amplitude processing techniques for marine, crystal-reflection seismic data: U.S. Geological Survey Bulletine 1897, 22 p.

Lee,M.W., Agena, W.F., and Swift, B.A., 1991, An analysis of a unique seismic anomaly in Georges Bank basin, Atlantic Continental Margin: U.S. Geological Survey Open-File Report 91-138, 25 p.

Lindseth. R.O., 1979, Synthetic sonic logs--a process for stratigraphic interpretation: Geophysics, v. 44, p. 3-26.

Markl, R.G., Bryan, G.M., and Ewing, J.I., 1970, Structure of the Blake-Bahama Outer Ridge: Journal of Geophysical Research, v. 75, p. 4539-4555.

McIver, R.D., 1981, Gas Hydrate, in Mayer, R.G. and Olson, J.C., eds., Long term energy resources, Pitman, Boston, p. 713-726.

Miller, J.J., Lee, M.W., and von Huene, R., 1991, An analysis of seismic reflection from the base of a gas hydrate zone, offshore Peru: American Association of Petroleum Geologists Bulletine, v. 75, p. 910-924.

Nobes, D.C., Villinger, H., Davis, F.F., and Law, L.K., 1986, Estimation of marine sediment bulk physical properties at depth from seafloor geophysical measurements: Journal of Geophysical Research, v. 91, p. 14033-14043.

Pandit, B.I., and King, M.S., 1983, Elastic wave velocities of propane gas hydrates, in Cox, J.L, ed., Natural gas hydrates: properties, occurrence and recovery, Butterworth Publishers, Boston, p. 49-61.

Paull, C.K., Ussler, W. Third, and Dillon, W.P., 1991, Is the extent of glaciation limited by marine gas hydrates?: Geophysical Research Letters, v. 18, p. 432-434.

Pearson, C.F., Halleck, P.M., McGulre, P.L., Hermes, R., and Mathews, M., 1983, Natural gas hydrate; a review of in situ properties: Journal of Physical Chemistry, v. 87, p. 4180-4185.

Sheridan, R.B., Gradstein, F.M., and others, 1983, Site Reports and underway data: Initial reports of the deep sea drilling project 76, p. 35-80.

Shipley, T.H., and Didyh, B.M., 1982, Occurrence of methane hydrates offshore southern Mexico: Initial Report of the Deep Sea Drilling Project 66, p. 547-556.

Shipley, T.H., Houston, M.H., Buffler, R.T., Shaub, F.J., McMillen, K.J., Ladd, J.W., and Worzel, J.L., 1979, Seismic evidence for widespread possible gas hydrate horizons on continental slopes and rises: American Association of Petroleum Geologists Bulletine, v. 63, p. 2204-2213.

Sloan, E.D., Jr., 1990, Clathrate hydrates of natural gases: Marcel Dekker, Inc., New York, 641 p.

Suess, E.R., von Huene, R. and others, 1988, Introduction, objectives, and principal results, LEG 112, Peru Continental Margin: Proceedings of the Ocean Drilling Program, initial reports 112, p. 5-44.

Timur, A., 1968; Velocity of compressional waves in porous media at permafrost temperature: Geophysics, v. 3, p. 584-595.

Tucholke, B.E., Bryan, G.M., and Ewing, J.I., 1977, Gas hydrate horizons detected in seismic-profile data from the western North Atlantic: American Association of Petroleum Geologists Bulletine, v. 61, p. 698-707.

Wyllie, M.R.J., Gregory, A.R., and Gardner, G.H.F., 1958, An experimental investigation of factors affecting elastic wave velocities in porous media: Geophysics, v. 23, p. 459-493.